

EDUCATIONAL REVIEW

Open Access

# Advanced imaging in adult diffusely infiltrating low-grade gliomas



Nail Bulakbaşı<sup>1\*</sup>  and Yahya Paksoy<sup>2</sup>

## Abstract

The adult diffusely infiltrating low-grade gliomas (LGGs) are typically IDH mutant and slow-growing gliomas having moderately increased cellularity generally without mitosis, necrosis, and microvascular proliferation. Supra-total resection of LGG significantly increases the overall survival by delaying malignant transformation compared with a simple debulking so accurate MR diagnosis is crucial for treatment planning. Data from meta-analysis support the addition of diffusion and perfusion-weighted MR imaging and MR spectroscopy in the diagnosis of suspected LGG. Typically, LGG has lower cellularity ( $ADC_{min}$ ), angiogenesis ( $rCBV_{max}$ ), capillary permeability ( $K_{trans}$ ), and mitotic activity (Cho/Cr ratio) compared to high-grade glioma. The identification of 2-hydroxyglutarate by MR spectroscopy can reflect the IDH status of the tumor. The initial low  $ADC_{min}$ , high  $rCBV_{max}$ , and  $K_{trans}$  values are consistent with the poor prognosis. The gradual increase in intratumoral Cho/Cr ratio and  $rCBV_{max}$  values are well correlated with tumor progression. Besides MR-based technical artifacts, which are minimized by the voxel-based assessment of data obtained by histogram analysis, the problems derived from the diversity and the analysis of imaging data should be solved by using artificial intelligence techniques. The quantitative multiparametric MR imaging of LGG can either improve the diagnostic accuracy of their differential diagnosis or assess their prognosis.

**Keywords:** Astrocytoma (grade II), Oligodendroglioma (adult), Magnetic resonance imaging

## Key points

- LGG has lower cellularity ( $ADC_{min}$ ), angiogenesis ( $rCBV_{max}$ ), capillary permeability ( $K_{trans}$ ), and mitotic activity (Cho/Cr) than HGG.
- Initial low  $ADC_{min}$  and high  $CBV_{max}$  and  $K_{trans}$  values are consistent with the poor prognosis.
- A gradual increase in Cho/Cr ratio and  $rCBV_{max}$  values is well-correlated with tumor progression.
- Critical distortions in quantifying parameters can be minimized by proper ROI selection and voxel-based assessment.
- Quantitative multiparametric MRI can either improve the diagnostic accuracy of conventional MRI or provide a better assessment.

## Introduction

According to the 2016 update of World Health Organization (WHO) on the classification of tumors of the central nervous system, diffusely infiltrating low-grade gliomas (LGG) in the adult include the WHO grade II astrocytoma and oligodendrogliomas but rarely oligoastrocytomas [1, 2]. Because most of the oligoastrocytomas have genetic profiles typical of either diffuse astrocytoma or oligodendroglioma and the new WHO classification discourages the diagnosis of tumors as oligoastrocytoma or mixed glioma [1, 2]. Typically, LGGs are slow-growing tumors having moderately increased cellularity without prominent mitosis, necrosis, and microvascular proliferation [1]. So they usually have more indolent clinical course than high-grade gliomas (HGG), included anaplastic astrocytoma (grade III), anaplastic oligodendroglioma (grade III), and glioblastoma (grade IV). Their incidence peaks are at an earlier age of life (third to fourth decades), as opposed to those of HGG (sixth to seventh decades) [1, 3]. The gliomas show diffuse infiltration of adjacent and distant brain structures that are largely irrespective of its histological grade

\* Correspondence: [nail.bulakbasi@kyrenia.edu.tr](mailto:nail.bulakbasi@kyrenia.edu.tr)

<sup>1</sup>Medical Faculty, University of Kyrenia, Sehat Yahya Bakir Street, Karakum, Mersin-10 Kyrenia, Turkish Republic of Northern Cyprus, Turkey  
Full list of author information is available at the end of the article

and even its low grade, it usually shows microscopic peritumoral white matter tract invasion [1]. The demonstration of this diffuse infiltration is very important for the accurate glioma diagnosis.

The precise diagnosis of LGG is critical to make an appropriate treatment decision, because the supra-total resection (defined as the removal of a margin around the tumor visible on FLAIR images) significantly increases the overall survival and delays the malignant transformation of LGG [4, 5]. The surgical biopsy is reserved in markedly diffuse lesions like a gliomatosis cerebri pattern [4]. Because of the lack of consensus among various diagnosis, management, and treatment options in LGG, the joint tumor section of the American Association of Neurological Surgeons and the Congress of Neurological Surgeons published the evidence-based guidelines in 2015 [6]. These include a systematic review as well as an evidence-based clinical practice guideline about the role of imaging in the management of adult diffusely infiltrating LGG [7].

Magnetic resonance imaging (MRI) is the modality of choice in the diagnostic assessment of LGG and provides a reasonably good delineation of the gliomas [5, 7]. The quantitative assessment of advanced MR imaging techniques has long been used both for the preoperative evaluation of gliomas by providing molecular and metabolic information in addition to the routine anatomical evaluation [7, 8]. There is also a significant role in follow-up particularly in the differentiation of the post-irradiation changes and of the pseudo-progression [7]. The quantitative multiparametric MRI approach can improve the diagnostic accuracy of conventional MRI [8]. In this educational review, we aim to define the spectrum and diagnostic value of the available advanced imaging techniques in neuro-oncology. We will also review the added value as well as the possible pitfalls of using quantitative MRI techniques in addition to conventional MRI. Finally, the review will assess the importance of advanced MRI acquisition technique standardization in clinical practice of neuro-oncology.

### Imaging technique

The multiparametric MRI evaluation of LGG includes the conventional anatomical MRI sequences, namely T2, fluid-attenuated inversion recovery (FLAIR) and pre- and post-contrast T1-weighted images. In addition, the protocol includes advanced MRI techniques such as susceptibility-weighted imaging (SWI), diffusion-weighted imaging (DWI), perfusion-weighted imaging (PWI), MRI spectroscopy (MRS), and functional MRI (fMRI) techniques. The T1 and FLAIR sequences should be preferred as volumetric acquisitions particularly for the follow-up to make an appropriate comparison about the tumor progression or the high-grade transformation of LGG [7].

The subtracted images of pre- and post-contrast 3D T1-weighted or FLAIR images provide a better assessment of tumoral enhancement. The SWI is quite important to identify the intratumoral calcifications, microbleeds, vasculature and allows the calculation of intratumoral susceptibility score (ITSS) [9]. The DWI and the calculation of apparent diffusion coefficient (ADC) should always be in the routine diagnostic protocol, but at present diffusion kurtosis imaging is usually reserved for research purposes. Dynamic susceptibility contrast (DSC) and/or dynamic contrast-enhanced (DCE) perfusion imaging techniques are crucial for both the initial diagnosis and the follow-up of LGG [7, 9, 10]. Arterial spin labeling (ASL) perfusion is an alternative perfusion technique, which uses the magnetically labeled water protons as a contrast material and can also be used for the same purposes but it does not allow the calculation of relative cerebral blood volume (rCBV) [11]. It is usually preferred in patients with previous severe allergic/anaphylactoid reaction to a gadolinium-based contrast agent; patients with severe renal disease (eGFR < 30 mL/min/1.73 m<sup>2</sup>) or acutely deteriorating renal function; patients who would be at risk of nephrogenic systemic fibrosis; and patients who are, or might be, pregnant [11, 12]. The MRS is usually reserved for diagnostic verification and problem solving but not for the routine diagnosis [7]. But recently, high-resolution MRS technique with selective TE and different editing method is being used in glioma diagnosis to detect 2-hydroxyglutarate (2-HG), which accumulates within the gliomas having isocitrate dehydrogenase 1 and 2 (IDH 1/2) mutations [13, 14]. Diffusion tensor imaging and tractography with or without fMRI are usually reserved for preoperative evaluation of selected cases. The new emerging MRI techniques, such as amide proton transfer (APT) imaging [15, 16], sodium MRI [17], and MR elastography [18] can also be used for glioma grading but they are usually reserved for research purposes.

### Radiomic data for the histopathological features of LGGs

According to guideline, conventional MRI is the first-order technique (Level II evidence) to identify the location of the tumor and its relation to adjacent cerebral structures [7]. The diffusion and perfusion images are quite helpful in the assessment of LGG (Level II, Class II/III evidence) by providing a better identification of tumoral heterogeneity than anatomic MRI sequences and provide the differential diagnosis for tumor subtype and grade [7]. The diagnostic potential of MRS and positron emission tomography (Level III, Class III evidence) are still being defined [7]. The data of radiologic-pathologic correlation from meta-analysis of current literature [10, 11, 15, 19–31] demonstrates that the tumoral cellularity correlates with low T2 signal and low ADC; atypia with

low ADC and high fractional anisotropy; mitotic activity with high Cho/Cr, Cho/NAA ratios, rCBV, and APT signal; the microvascular proliferation with high rCBV, volume transfer coefficient ( $K_{trans}$ ), volume fraction of plasma ( $V_p$ ), and ITSS; and necrosis with necrotic cavity and high lactate levels on MR spectroscopy.

The differential diagnosis and grading of gliomas are still debating. The quantitative multiparametric MR imaging approach can better differentiate LGG from HGG with very high sensitivity (84.2%), and specificity (100%) than conventional MRI, thereby reducing the risk of inappropriate or delayed surgery, respectively [8]. By this purpose, a significant amount of quantitative data has been collected during the last decade and a lot of different cut-off values have been defined for the grading of gliomas in the literature as summarized in Table 1 [7, 9–11, 19–30]. The most common parameters defined in literature for grading are maximum relative cerebral blood volume ( $rCBV_{max}$ ), minimum normalized ADC ( $nADC_{min}$ ), and choline to creatine (Cho/Cr) ratio. The defined cut-off values for glioma grading are 1.75 for  $rCBV_{max}$  in the largest cohort [19] ranging between 0.94 and 3.34 [9–11, 19–22],  $1.07 \times 10^{-3} \text{ mm}^2/\text{s}$  for  $nADC_{min}$  in the largest cohort [24] ranging between 0.31 and 1.31 [23–28] and 1.56 for Cho/Cr ratio in the largest cohort [19] ranging between 1.3 and 2.04 [29–31]. There was a considerable variation

in cut-off values because of the difference in the study design, types of MRI devices, coils, sequences, post-processing algorithms, picking up hot points vs. histogram analysis, and diverse methodology in determining cut-off values. A standardized, multicenter acquisition and analysis protocol for the imaging data is feasible and highly reproducible, having a comparable high diagnostic accuracy in glioma grading according to the new WHO 2016 classification scheme [21].

Typically, LGG has lower cellular density than HGG so has a higher  $ADC_{min}$  and minimum mean diffusivity, and lower fractional anisotropy and mean kurtosis values than HGG [23–28]. The optimal threshold was  $0.98 \times 10^{-3} \text{ mm}^2/\text{s}$  for  $ADC_{min}$  and 0.17 for the mean difference in mean kurtosis [26, 28]. The LGG has lower perfusion parameters such as  $K_{trans}$ , volume fraction of extravascular extracellular space ( $V_e$ ), mean vascular density, and  $rCBV_{max}$  values than HGG [9, 10, 19, 22]. This is primarily due to the fact that they are less prone to secrete vascular endothelial growth factor, having low microvascular proliferation and lack of immature, hyperpermeable neo-microvasculature [9, 10, 19, 22]. The  $rCBV_{max}$  threshold of 1.76 has the highest diagnostic accuracy for diffuse astrocytoma [10]. The LGG has also a lower maximum mean relative tumor blood flow/normal white matter ratio [11] and relatively lower ITSS degrees [9] than HGG, primarily due to a lack of tortuous, disorganized, dilated, and leaky tumoral capillaries. The LGG has significantly lower Cho/Cr or Cho/N-acetyl aspartate (NAA) ratios and higher myoinositol to Cr ratio than HGG due to having lower membrane turnover rates and production of proteolytic enzymes [29, 30]. LGG has a significantly lower APT signal intensity than HGGs [15, 16]. There is not a meaningful change in protein content of tumor and a moderate correlation between APT signal intensity and Ki-67 proliferation index [14]. Histogram analysis of APT imaging provides increased accuracy for the identification of contrast-enhancing LGG that mimics HGG [16].

Perfusion and diffusion images may also play a role (Level III) in consideration of tumor prognosis and in distinguishing different classes of LGG in terms of prognosis [7]. Poor outcome is well correlated with low  $ADC_{min}$  values ranging between  $0.799 \times 10^{-3} \text{ mm}^2/\text{s}$  and  $1.69 \times 10^{-3} \text{ mm}^2/\text{s}$  [32–34], high  $rCBV_{max}$  values ranging between 1.46 and 5.195 [32, 33, 35] and high permeability with  $K_{trans}$  values more than  $0.05 \text{ min}^{-1}$  and  $V_p$  values more than 5 ml/100 g [36].

In determining high-grade transformation, anatomical MRI (level II) is the first-order technique [7]. New contrast enhancement and increase in tumor size more than 3 mm per year may signify a transformation to a higher grade [7, 37]. Serial PWI and MRS (level III) are also

**Table 1** Radiomic data for differential diagnosis of low-grade vs high-grade gliomas

Parameters	Low-grade glioma	High-grade glioma	Cut of value [Ref] (range) [Ref]
$rCBV_{max}$	Low	High	1.76 [10, 19] (0.94–3.34) [9–11, 19–22]
$rCBV_{MD}$	Low	High	1.44 [22] (1.08–1.81) [22]
$nADC_{min}$	High	Low	$1.07 \times 10^{-3} \text{ mm}^2/\text{s}$ [24] (0.31–1.31) [23–28]
Cho/Cr ratio	Low	High	1.56 [19] (1.3–2.04) [29–31]
$MK_{MD}$	Low	High	0.17 [28] (0.11–0.28) [28]
$FA_{TC}$	Low	High	0.3 [25] (0.14–0.63) [25]
$MD_{min}$	High	Low	$0.98 \text{ mm}^2/\text{s}$ [25] (0.76–0.91) [25]
$k_{trans}$	High	Low	1.18 [22] (0.91–1.45) [22]
$V_e$	High	Low	1.43 [22] (1.06–1.80) [22]
ITTS grade	1.2	2.6	NA [9]
APT signal (%)	Low	High	2.23% [15] (1.53%–3.70%) [15]

$rCBV_{max}$  maximum relative cerebral blood volume,  $rCBV_{MD}$  standardized mean difference of  $rCBV_{max}$ ,  $nADC_{min}$  normalized minimum apparent diffusion coefficient, Cho/Cr choline/creatine,  $MK_{MD}$  mean difference in mean kurtosis,  $FA_{TC}$  odds ratio of fractional anisotropy in the tumor core,  $MD_{min}$  minimum mean diffusivity,  $k_{trans}$  standardized mean difference of volume transfer coefficient,  $V_e$  standardized mean difference of volume fraction of extravascular extracellular space, ITTS intratumoral susceptibility score, APT percent amide proton transfer signal

useful for astrocytic tumors, baseline, and gradual longitudinal elevations in  $rCBV_{max}$  values and Cho/Cr ratios are associated with shorter time to tumor progression [7]. However, these can be difficult to standardize in clinical practice for oligodendrogliomas and mixed gliomas. Higher growth rate more than 3 mm per year [37], higher baseline  $rCBV_{max}$  values more than 1.52–1.75 [37–39] and higher Cho/Cr ratio more than 2.4 [37] are well correlated with high-grade transformation. In transforming LGG, a significant increase in  $rCBV_{max}$  can occur up to 12 months before contrast enhancement becomes apparent on T1-weighted MR images [39] and a significant increase in Cho/Cr ratio can occur up to 15 months before the  $rCBV_{max}$  elevation [37].

### Radiomic data for the genetic and molecular features of LGGs

According to the updated WHO 2016 classification, 75–80% of grade II diffusely infiltrating astrocytomas have IDH1/2 mutation and 20–25% do not [1, 3]. An IDH1/2 mutant diffusely infiltrating astrocytoma has also had a loss of nuclear alpha-thalassemia/mental retardation syndrome X-linked expression (ATRX) status and TP53 mutations [1, 3]. Although WHO 2016 is based on the basis of combined phenotypic and genotypic classification as well as the generation of integrated diagnoses, WHO grading of gliomas remained unchanged [1]. Essentially LGG has mild nuclear atypia, moderate pleomorphism, high degree of cellular differentiation, and low MIB-1, with intrinsic capacity to progress to IDH1 mutant anaplastic astrocytoma or glioblastoma [1, 3].

There is a big survival difference between IDH1-mutated vs. wild-type gliomas. Although IDH1 mutant glioblastoma has still significantly worse outcomes than grade II and III gliomas, there are no differences in survival between IDH mutant grades II and III [40]. For this reason, Shirahata et al. proposed a novel, improved grading system for IDH-mutant astrocytic gliomas [41]. The premise is cyclin-dependent kinase Inhibitor 2A/B homozygous deletion with combination of necrosis and copy number variation has the most relevant results for survival but the proliferation (mitotic count) has only a minor influence on survival [41].

The IDH mutant LGG is usually located in the frontal lobe followed by temporal lobe and infratentorial location (Fig. 1). They are mostly solid and do not enhance. They have usually well-defined border and T2/FLAIR “mismatch” sign represented as homogeneous high signal on T2 sequence but bright rim and dark center on FLAIR images [42]. Typically, they have higher  $ADC_{min}$  and lower  $rCBV_{max}$  values than wild-type tumors and are represented with a slight increase in Cho/NAA as well as Cho/Cr ratios [10, 42, 43]. Radiomic features extracted from the optimal texture analysis of ADC and

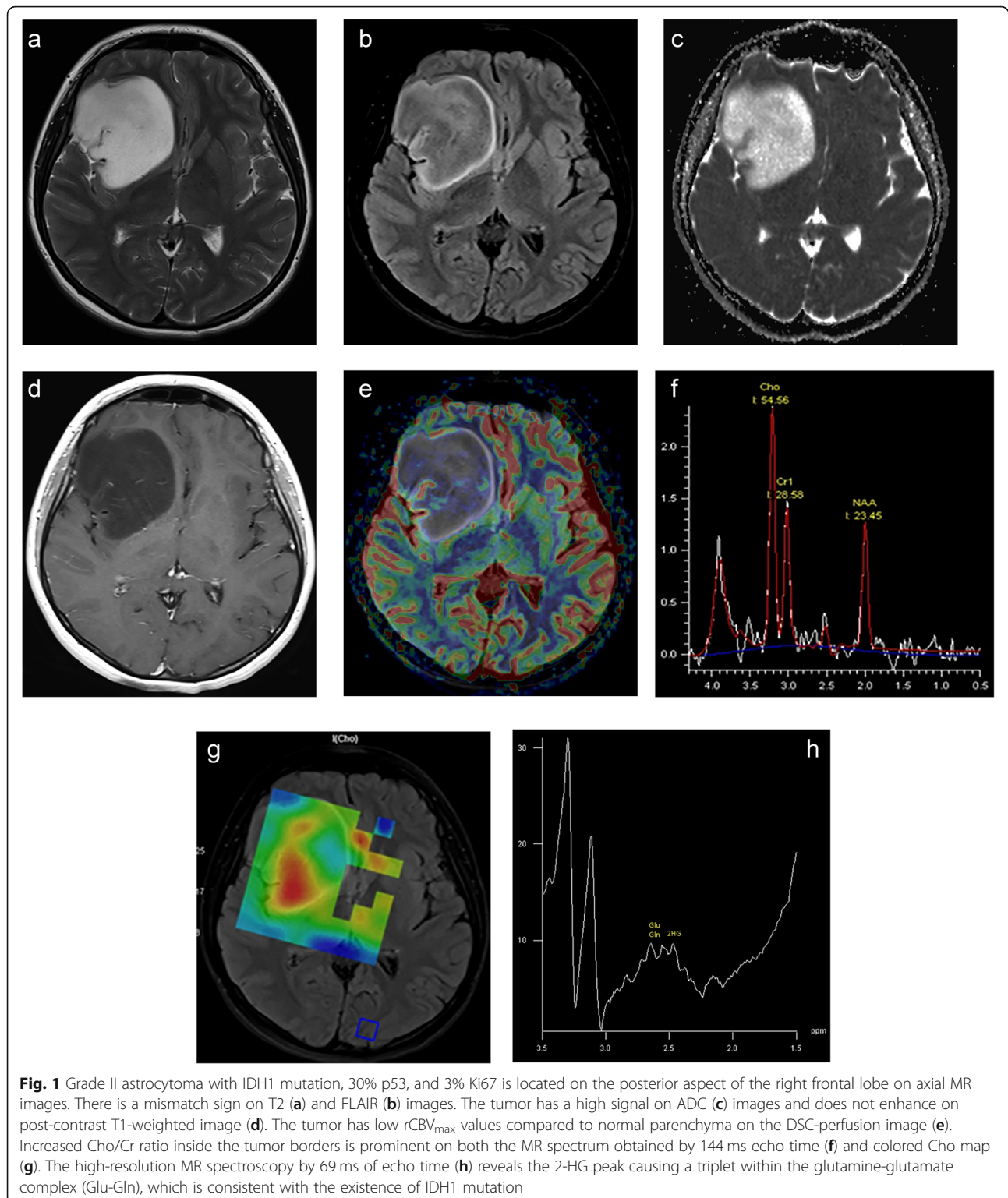
T2 FLAIR images play an important role in the noninvasive prediction of the IDH1 mutation and loss of ATRX expression status in LGGs [43]. Choi and colleagues showed the existence of 2-HG and glutamate multiplets in patients with IDH-mutated grade II-III tumors, with 100% sensitivity and specificity [13].

IDH-wild-type LGGs may not have been demonstrated because imaging and histopathology features look low grade, but molecular and clinical features suggest an early stage of primary glioblastoma [44]. Recent literature recommends the use of diffuse astrocytic glioma, IDH-wild-type, with molecular features of glioblastoma, WHO grade IV a.k.a. “Molecular GBM” diagnosis [45]. This is basically based on the existence of epidermal growth factor amplification or combined whole chromosome 7 gain, whole chromosome 10 loss (+7/-10) or telomerase reverse transcriptase promoter mutation, regardless of its histological WHO grade [45]. IDH wild-type diffuse astrocytomas are more likely to exhibit contrast enhancement with intratumoral necrosis and peritumoral edema, but not cyst (Fig. 2). The  $ADC_{mean}$  of 1.2 can be used as an optimal cutoff value to differentiate IDH wild-type and IDH-mutant gliomas irrespective of WHO grade and tumors with  $ADC_{mean}$  less than 1.08 had poor survival [46]. The absence of a 2-HG peak in MR spectroscopy is also consistent with the IDH wild-type tumors [13, 14]. Furthermore, recent literature also demonstrates that IDH-mutated astrocytomas have higher ADC [46–48] and lower  $rCBV$  values [47–49], an APT signal [15, 16], the relaxation-weighted sodium signal to total sodium signal ratio [17], oxygen extraction fraction [50], and tumor stiffness [18] than IDH wild-type tumors.

According to WHO 2016 update, diffusely infiltrating oligodendroglioma (Fig. 3) is a slow-growing glioma with IDH1 or IDH2 mutation and codeletion of chromosomal arms 1p and 19q (1p19q-codeletion) [1]. They have higher  $rCBV$  and  $V_e$  and lower  $ADC_{mean}$  values than the same grade diffusely infiltrating astrocytomas because of having a chicken wire-fine capillary network causing higher tissue perfusion even in grade II [51–57]. Higher  $V_e$  values are usually with the presence of cortical involvement and calcification and/or hemorrhage [53]. The  $rCBV$  ratio, greater than 1.6 is predictive of the 1p19q-codeleted genotype with 92% sensitivity and 76% specificity [54]. Cho/Cr ratio had the highest predictive value, with moderate accuracy (69%) when combined with  $rCBV_{max}$  [55]. They have also higher ITSS than the same grade diffuse astrocytomas due to increased angiogenesis, dense vascularity, microbleeds, or microcalcifications [52].

### Possible pitfalls and solutions

The first problem preventing a proper data quantification are MRI artifacts, which are mainly related to



magnetic field like susceptibility or inhomogeneity artifacts, or to patient caused by (in)voluntary motion, blood flow, or cerebrospinal fluid pulsation [58, 59]. The magnetic field-based distortions can be reduced by using less

sensitive pulse sequences, shorter TE values, wider receiver bandwidths or by applying parallel imaging techniques, and patient-based artifacts can be eliminated by proper immobilization and gating techniques [58, 59].

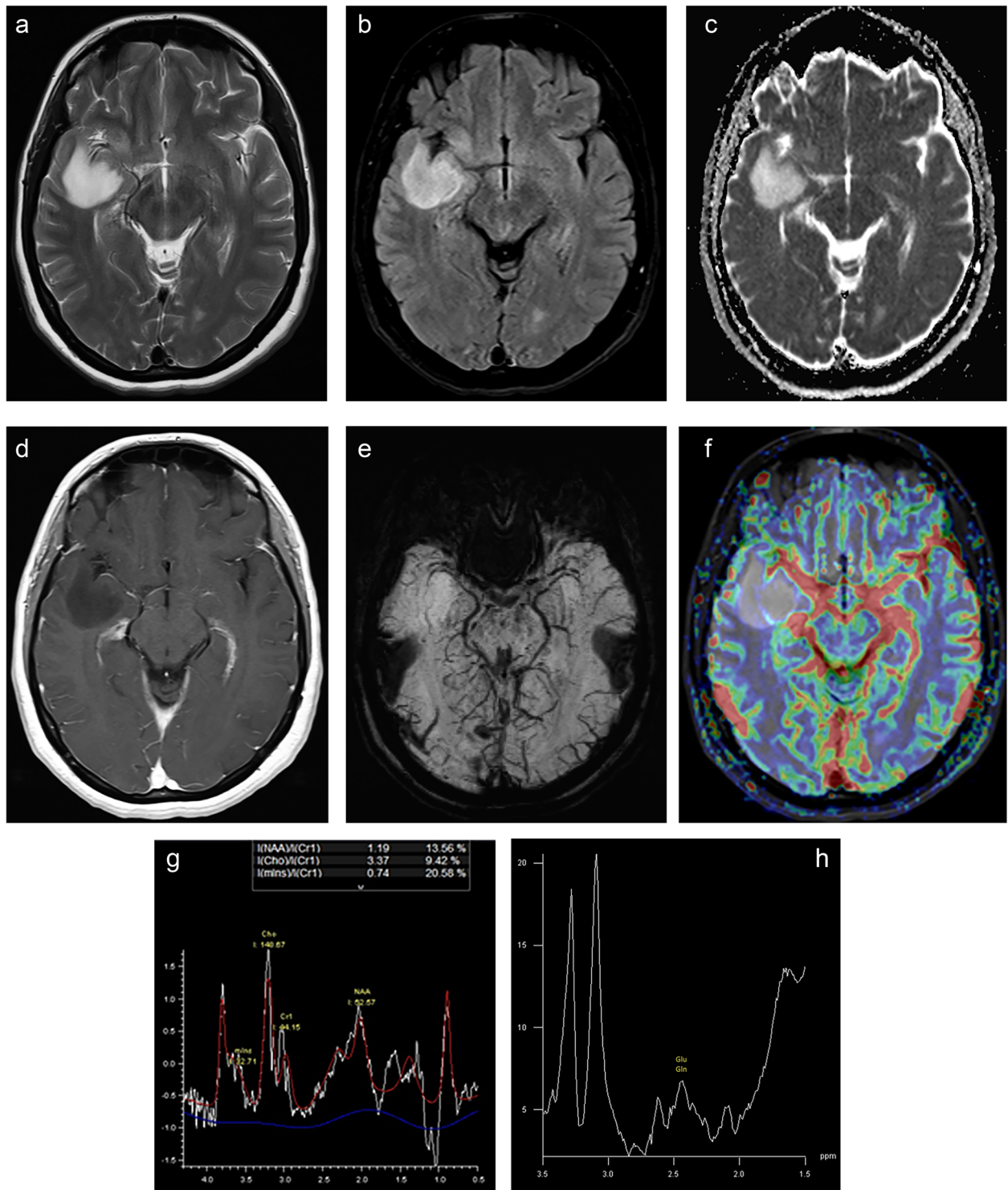


**Fig. 2** Astrocytoma, grade II with the absence of IDH1 mutation (IDH wild-type), loss of ATRX expression, 20% p53, and 3.3% Ki67 is located on the right temporal lobe on axial MR images. The tumor has a high signal on T2 (a), FLAIR (b), and ADC (c) images and faint enhancement on post-contrast T1-weighted image (d). The tumor has low ITSS on SW image (e) and rCBV<sub>max</sub> values compared to normal parenchyma on the DSC-perfusion image (f). The tumor has increased Cho/Cr ratio and low NAA/Cr ratio on the MR spectrum obtained by 144 ms echo time (g). The high-resolution MR spectroscopy by 69 ms of echo time (h) reveals a singlet due to the glutamine-glutamate complex (Glu-Gln), which is consistent with the absence of 2-HG peak and IDH1 mutation

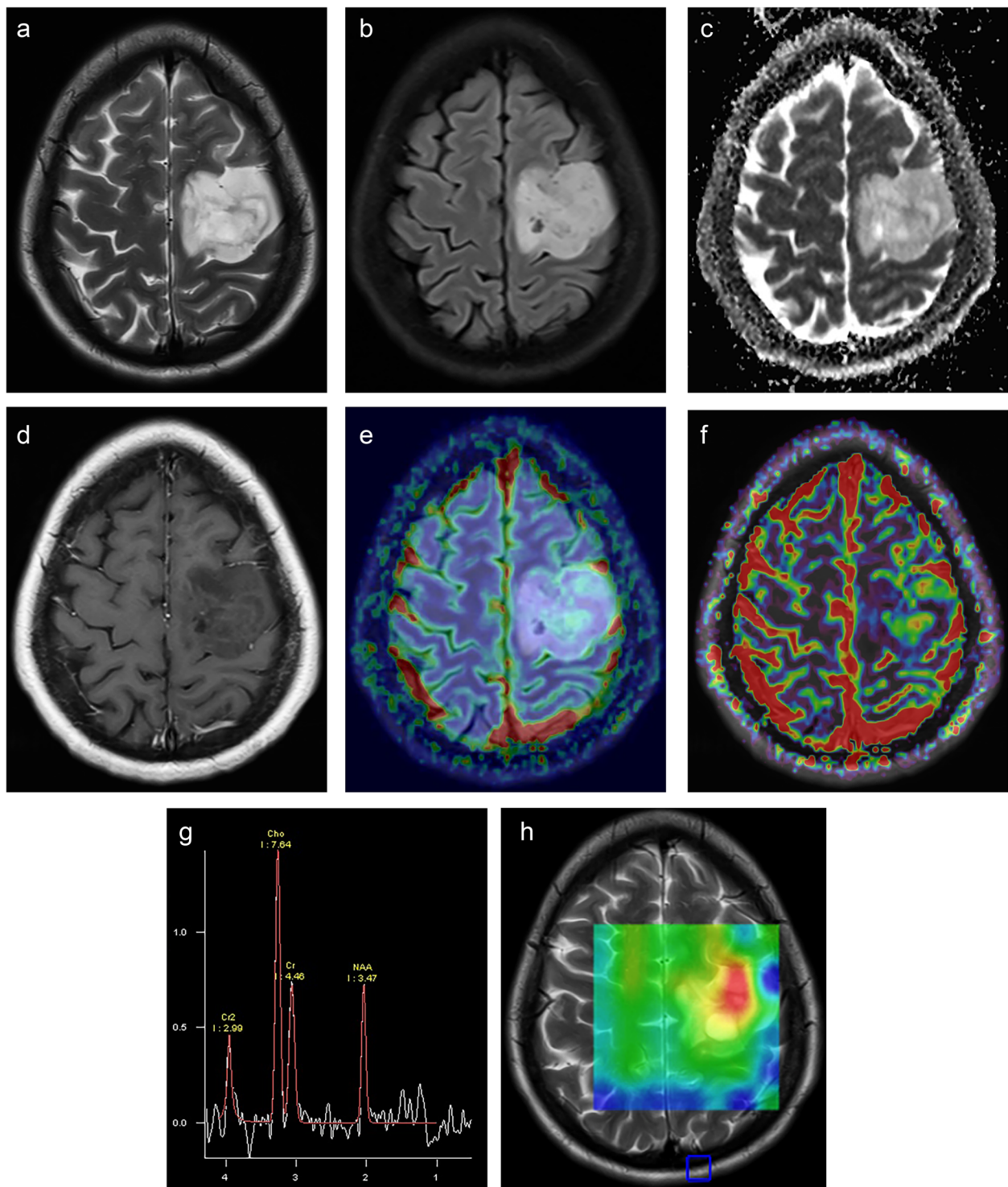


**Fig. 3** Oligodendroglioma, grade II with 1p19q-codeletion, intact ATRX expression, immune-negative p53, and 2% Ki67 is located on the premotor area of the left frontal lobe on axial MR images. The irregularly contoured tumor has a heterogeneous high signal on T2 (a), FLAIR (b), and ADC (c) images and has a central intratumoral small low signal area consistent with calcification/hemorrhage. It has faint enhancement on post-contrast T1-weighted image (d). The tumor has relatively higher  $rCBV_{max}$  values than normal parenchyma on DSC-perfusion image (e) and  $k_{trans}$  values on DCE-perfusion image (f). The tumor has also high Cho/Cr ratio on the MR spectrum obtained by 144 ms echo time (g) at the similar areas of increased perfusion on colored Cho map (h)

Small tumor diameter and vascular structures, hemorrhagic, cystic/necrotic, and calcific changes in the tumoral area can also cause critical distortions in quantifying parameters. So the selection of a proper

region of interest (ROI) avoiding this kind of areas or the use of histogram analysis can minimize these distortive effects (Fig. 4). The usage of histogram analysis, compared with the use of the current hotspot

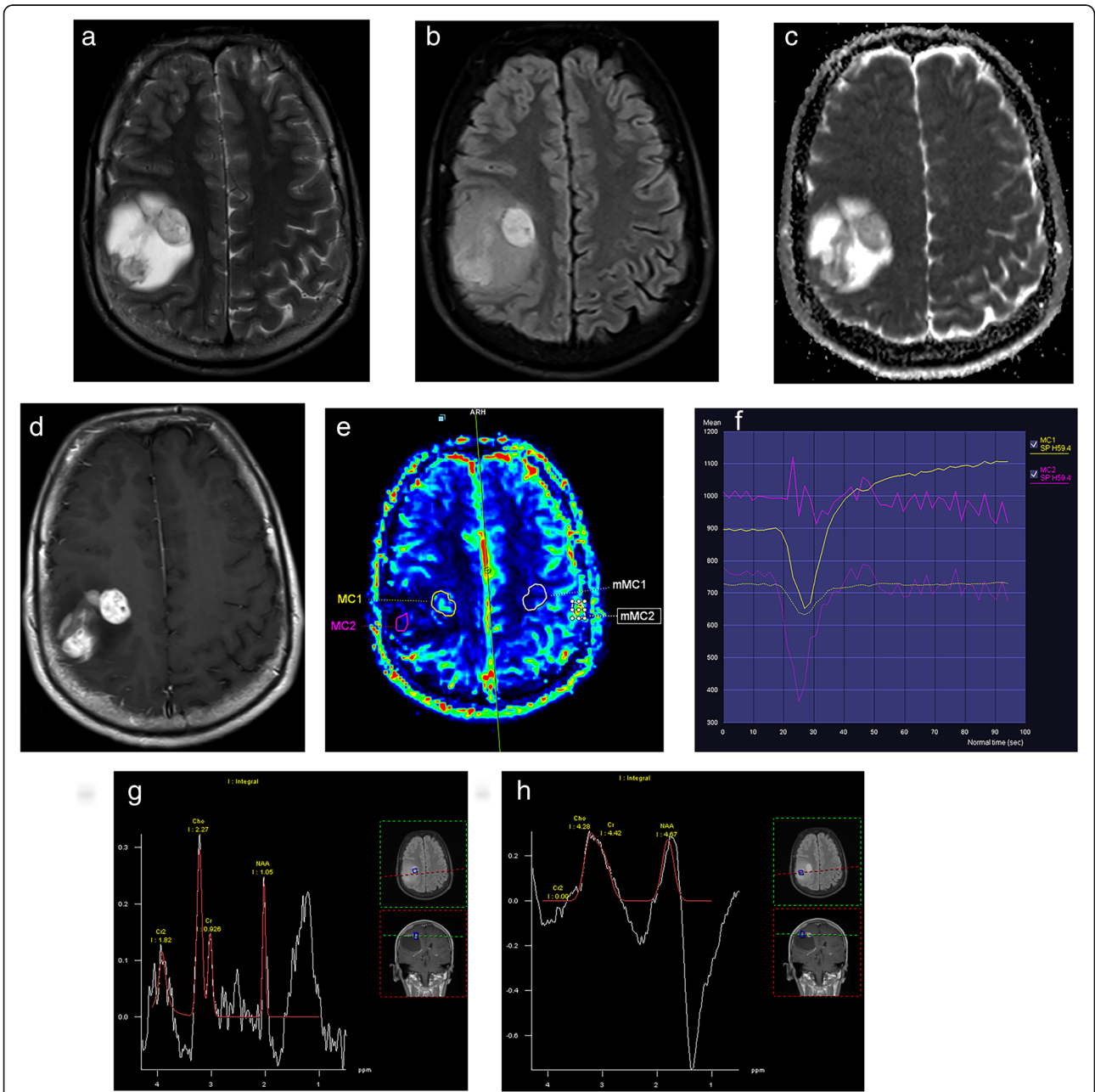


**Fig. 4** Pilocytic astrocytoma, grade I with immune-negative IHD-1, CD138 and Neu N, and 1% Ki67 is located on the right fronto-parietal lobe on axial MR images. The lobulated but regularly contoured tumor has cystic and solid components on T2 (a) and FLAIR (b) images and relatively low ADC values (c). The solid components of the tumor have heterogenous enhancement on post-contrast T1-weighted image (d). On DSC-perfusion image (e) two ROIs picked areas showing strong (MC1) and weak (MC2) enhancement and their mirrored counterpart areas (mMC1 and mMC2) from normal parenchyma. The perfusion signal to time graph (f) shows increased perfusion curve on MC1 tumoral core (solid yellow curve) compared to mMC1 normal parenchyma curve (dotted yellow curve) but distorted irregular curve on MC2 weakly enhanced area (pink solid curve) due to partial volume effect of cystic component of tumor causing erroneous rCBV values. Similarly, while MR spectrum obtained by 144 ms echo time from MC1 region (g) is consistent with tumoral spectrum with increased Cho/Cr ratio and decreased NAA, the MR spectra from MC2 region (h) show distorted and unrecognizable curves due to the same reason



technique, can increase the diagnostic accuracy and the interobserver reproducibility in glioma grading as well as potentially improve patient care [56, 57]. Also emerging AI algorithms can provide the voxel-based assessment of data obtained by histogram analysis or other methods. The voxel-based assessment of imaging data provides new quantitative information, which is invisible to human assessment and can more precisely extract and use thousands of different and new radiomic features, which are validated as the quantitative imaging biomarkers to characterize intratumoral dynamics throughout diagnosis and treatment [60–63]. The second problem is the analysis of data. Recent multiparametric MRI techniques produce a significant amount of imaging data with massive diversity from patient to patient. The analysis and post-processing of this large volume of data is not only complex and time-consuming but also lacks standardization. The newly emerging AI techniques using diagnostic hypotheses and scalable machine-learning algorithms have the potential of automated processing of large data volumes and can enhance the current performance of quantitative cancer imaging [63]. Providing standardization is more difficult because of the variety of hardware and software produced by different vendors, mostly makes the exact comparison of the results difficult. Also, the differences in the scanner type, magnetic field strength, acquisition parameters, protocols, and determination of standard threshold levels make this comparison less reliable. The standardized, multicenter acquisition and analysis protocols can generate more feasible and highly reproducible data and increase the diagnostic accuracy [21]. The AI algorithms using the data mined by machine-learning methods can help to minimize the effects caused by lack of standardization resulting in more reliable results.

## Conclusion

The parameters obtained from the quantification of multiparametric brain MRI can provide an adequate diagnosis of LGG and help to differentiate them from HGG. The LGG has a lower cellularity ( $ADC_{min}$ ), angiogenesis ( $rCBV_{max}$ ), capillary permeability ( $K_{trans}$ ), and mitotic activity (Cho/Cr) than HGG. Besides these basic parameters, thousands of different and new radiomic features have been defined in the literature and more will continue to emerge with the advent of AI techniques. The initial low  $ADC_{min}$  values, high  $rCBV_{max}$ , and  $K_{trans}$  values are consistent with the poor prognosis. The gradual increase in intratumoral Cho/Cr ratio and  $rCBV_{max}$  values are well correlated with tumor progression. The major problems in the quantitative multiparametric MR imaging of LGGs include the diversity of

imaging equipment and techniques. This can be minimized by using a comparable standardized, multicenter acquisition and analysis protocols and the analysis of large volume data, which can be solved by the automated processing methods of AI. The radiomic features obtained by quantitative multiparametric MRI can enhance the current performance and the clinical potential of a predictive cancer diagnosis.

## Abbreviations

2-HG: 2-hydroxy-glutarate; ADC: Apparent diffusion coefficient; AI: Artificial intelligence; APT: Amide proton transfer; ASL: Arterial spin labeling; Cho: Choline; Cr: Creatine; DCE: Dynamic contrast-enhanced; DSC: Dynamic susceptibility contrast; DWI: Diffusion-weighted imaging; FLAIR: Fluid-attenuated inversion recovery; fMRI: Functional MRI; HGG: High-grade glioma; IDH: Isocitrate dehydrogenase; ITSS: Intratumoral susceptibility score;  $K_{trans}$ : Volume transfer coefficient; LGG: Low-grade glioma; MRI: Magnetic resonance imaging; MRS: MRI spectroscopy; NAA: n-acetyl aspartate; PWI: Perfusion-weighted imaging; rCBV: Relative cerebral blood volume; SWI: Susceptibility-weighted imaging;  $V_e$ : Volume fraction of extravascular extracellular space;  $V_p$ : Volume fraction of plasma; WHO: World Health Organization

## Acknowledgments

This article was presented at ECR 2018 and ECR 2019 as an invited lecture. It is about an update of advanced MR imaging techniques in the diagnosis and follow-up of adult diffusely infiltrating low-grade gliomas.

## Authors' contributions

NB prepared, read, and approved the final manuscript. YP contributed to patient data, and read and approved the final manuscript.

## Funding

The authors declare that this work has not received any funding.

## Availability of data and materials

The datasets used and/or analyzed during the current study are available from the corresponding author on reasonable request.

## Ethics approval and consent to participate

This educational review includes a statement on ethics approval and consent from the ethic committee of University of Kyrenia, dated on August 8, 2019, and numbered as 2019/01–016.

## Consent for publication

The selected pictures of sample cases have personal consent form of each patient.

## Competing interests

The authors declare that they have no competing interests.

## Author details

<sup>1</sup>Medical Faculty, University of Kyrenia, Sehit Yahya Bakir Street, Karakum, Mersin-10 Kyrenia, Turkish Republic of Northern Cyprus, Turkey. <sup>2</sup>Selcuk University, Konya, Turkey.

Received: 12 August 2019 Accepted: 25 September 2019

Published online: 18 December 2019

## References

- Louis DN, Ohgaki H, Wiestler OD, Cavenee WK (2016) WHO classification of tumours of the central nervous system, revised 4th edition. IARC, Lyon
- Sahm F, Reuss D, Koelsche C et al (2014) Farewell to oligoastrocytoma: in situ molecular genetics favor classification as either oligodendroglioma or astrocytoma. *Acta Neuropathol* 128(4):551–559. <https://doi.org/10.1007/s00401-014-1326-7>
- Bready D, Placantonakis DG (2019) Molecular pathogenesis of low-grade glioma. *Neurosurg Clin N Am* 30(1):17–25. <https://doi.org/10.1016/j.nec.2018.08.011>

4. Duffau H (2016) Long-term outcomes after supratotal resection of diffuse low-grade gliomas: a consecutive series with 11-year follow-up. *Acta Neurochir (Wien)* 158(1):51–58. <https://doi.org/10.1007/s00701-015-2621-3>
5. National Comprehensive Cancer Network. Central nervous system cancers (Version 1.2019). [https://www.nccn.org/professionals/physician\\_gls/pdf/cns.pdf](https://www.nccn.org/professionals/physician_gls/pdf/cns.pdf). Accessed Mar 5 2019
6. Olson JJ, Kalkanis SN, Ryken TC (2015) Evidence-based clinical practice parameter guidelines for the treatment of adults with diffuse low-grade glioma: introduction and methods. *J Neurooncol* 125(3):449–456. <https://doi.org/10.1007/s11060-015-1847-5>
7. Fouke SJ, Benzinger T, Gibson D, Ryken TC, Kalkanis SN, Olson JJ (2015) The role of imaging in the management of adults with diffuse low-grade glioma: a systematic review and evidence-based clinical practice guideline. *J Neurooncol* 125(3):457–479. <https://doi.org/10.1007/s11060-015-1908-9>
8. Caulo M, Panara V, Tortora D et al (2014) Data-driven grading of brain gliomas: a multiparametric MR imaging study. *Radiology* 272(2):494–503. <https://doi.org/10.1148/radiol.14132040>
9. Li X, Zhu Y, Kang H et al (2015) Glioma grading by microvascular permeability parameters derived from dynamic contrast-enhanced MRI and intratumoral susceptibility signal on susceptibility weighted imaging. *Cancer Imaging* 15:4. <https://doi.org/10.1186/s40644-015-0039-z>
10. Delgado AF, Delgado AF (2017) Discrimination between glioma grades II and III using dynamic susceptibility perfusion MRI: a meta-analysis. *AJNR Am J Neuroradiol* 38(7):1348–1355. <https://doi.org/10.3174/ajnr.A5218>
11. Kong L, Chen H, Yang Y, Chen L (2017) A meta-analysis of arterial spin labelling perfusion values for the prediction of glioma grade. *Clin Radiol* 72(3):255–261. <https://doi.org/10.1016/j.crad.2016.10.016>
12. ACR Committee on Drugs and Contrast Media (2018) ACR manual on contrast media (Version 10.3, 2018). [https://www.acr.org/-/media/ACR/Files/Clinical-Resources/Contrast\\_Media.pdf](https://www.acr.org/-/media/ACR/Files/Clinical-Resources/Contrast_Media.pdf). Accessed 2018
13. Choi C, Ganji SK, DeBerardinis RJ et al (2012) 2-hydroxyglutarate detection by magnetic resonance spectroscopy in IDH-mutated patients with gliomas. *Nat Med* 18(4):624–629. <https://doi.org/10.1038/nm.2682>
14. Tietze A, Choi C, Mickey B et al (2018) Noninvasive assessment of isocitrate dehydrogenase mutation status in cerebral gliomas by magnetic resonance spectroscopy in a clinical setting. *J Neurosurg* 128(2):391–398. <https://doi.org/10.3171/2016.10.JNS161793>
15. Suh CH, Park JE, Jung SC, Choi CG, Kim SJ, Kim HS (2019) Amide proton transfer-weighted MRI in distinguishing high- and low-grade gliomas: a systematic review and meta-analysis. *Neuroradiology* 61(5):525–534. <https://doi.org/10.1007/s00234-018-02152-2>
16. Park JE, Kim HS, Park KJ, Choi CG, Kim SJ (2015) Histogram analysis of amide proton transfer imaging to identify contrast-enhancing low-grade brain tumor that mimics high-grade tumor: increased accuracy of MR perfusion. *Radiology* 277(1):151–161. <https://doi.org/10.1148/radiol.2015142347>
17. Biller A, Badde S, Nagel A et al (2016) Improved brain tumor classification by sodium MR imaging: prediction of IDH mutation status and tumor progression. *AJNR Am J Neuroradiol* 37(1):66–73. <https://doi.org/10.3174/ajnr.A4493>
18. Pepin KM, McGee KP, Arani A et al (2018) MR elastography analysis of glioma stiffness and IDH1-mutation status. *AJNR Am J Neuroradiol* 39(1):31–36. <https://doi.org/10.3174/ajnr.A5415>
19. Law M, Yang S, Wang H et al (2003) Glioma grading: sensitivity, specificity, and predictive values of perfusion MR imaging and proton MR spectroscopic imaging compared with conventional MR imaging. *AJNR Am J Neuroradiol* 24(10):1989–1998
20. Bulakbasi N, Kocaoglu M, Farzaliyev A, Tayfun C, Ucoz T, Somuncu I (2005) Assessment of diagnostic accuracy of perfusion MR imaging in primary and metastatic solitary malignant brain tumors. *AJNR Am J Neuroradiol* 26(9):2187–2199
21. Anzalone N, Castellano A, Cadioli M et al (2018) Brain gliomas: multicenter standardized assessment of dynamic contrast-enhanced and dynamic susceptibility contrast MR images. *Radiology* 287(3):933–943. <https://doi.org/10.1148/radiol.2017170362>
22. Liang J, Liu D, Gao P et al (2018) Diagnostic values of DCE-MRI and DSC-MRI for differentiation between high-grade and low-grade gliomas: a comprehensive meta-analysis. *Acad Radiol* 25(3):338–348. <https://doi.org/10.1016/j.acra.2017.10.001>
23. Bulakbasi N, Guvenc I, Onguru O, Erdogan E, Tayfun C, Ucoz T (2004) The added value of the apparent diffusion coefficient calculation to magnetic resonance imaging in the differentiation and grading of malignant brain tumors. *J Comput Assist Tomogr* 28(6):735–746
24. Server A, Kulle B, Gadmar ØB, Josefsen R, Kumar T, Nakstad PH (2011) Measurements of diagnostic examination performance using quantitative apparent diffusion coefficient and proton MR spectroscopic imaging in the preoperative evaluation of tumor grade in cerebral gliomas. *Eur J Radiol* 80(2):462–470. <https://doi.org/10.1016/j.ejrad.2010.07.017>
25. Miloshevs VZ, Chow DS, Filippi CG (2015) Meta-analysis of diffusion metrics for the prediction of tumor grade in gliomas. *AJNR Am J Neuroradiol* 36(2):302–308. <https://doi.org/10.3174/ajnr.A4097>
26. Zhang L, Min Z, Tang M, Chen S, Lei X, Zhang X (2017) The utility of diffusion MRI with quantitative ADC measurements for differentiating high-grade from low-grade cerebral gliomas: evidence from a meta-analysis. *J Neurol Sci* 373:9–15. <https://doi.org/10.1016/j.jns.2016.12.008> Erratum in: *J Neurol Sci*. 2017;375:103-106
27. Liang R, Wang X, Li M et al (2014) Potential role of fractional anisotropy derived from diffusion tensor imaging in differentiating high-grade gliomas from low-grade gliomas: a meta-analysis. *Int J Clin Exp Med* 7(10):3647–3653
28. Falk Delgado A, Nilsson M, van Westen D, Falk Delgado A (2018) Glioma grade discrimination with MR diffusion kurtosis imaging: a meta-analysis of diagnostic accuracy. *Radiology* 287(1):119–127. <https://doi.org/10.1148/radiol.2017171315>
29. Castillo M, Smith JK, Kwock L (2000) Correlation of myo-inositol levels and grading of cerebral astrocytomas. *AJNR Am J Neuroradiol* 21(9):1645–1649
30. Wang Q, Zhang H, Zhang J et al (2016) The diagnostic performance of magnetic resonance spectroscopy in differentiating high-from low-grade gliomas: a systematic review and meta-analysis. *Eur Radiol* 26(8):2670–2684. <https://doi.org/10.1007/s00330-015-4046-z>
31. Usinskiene J, Ulyte A, Bjørnerud A et al (2016) Optimal differentiation of high- and low-grade glioma and metastasis: a meta-analysis of perfusion, diffusion, and spectroscopy metrics. *Neuroradiology* 58(4):339–350. <https://doi.org/10.1007/s00234-016-1642-9>
32. Hilario A, Sepulveda JM, Perez-Núñez A et al (2014) A prognostic model based on preoperative MRI predicts overall survival in patients with diffuse gliomas. *AJNR Am J Neuroradiol* 35(6):1096–1102. <https://doi.org/10.3174/ajnr.A3837>
33. Cuccarini V, Erbetta A, Farinotti M et al (2016) Advanced MRI may complement histological diagnosis of lower grade gliomas and help in predicting survival. *J Neurooncol* 126(2):279–288
34. Villanueva-Meyer JE, Wood MD, Choi BS et al (2018) MRI features and IDH mutational status of grade II diffuse gliomas: impact on diagnosis and prognosis. *AJR Am J Roentgenol* 210(3):621–628. <https://doi.org/10.2214/AJR.17.18457>
35. Law M, Oh S, Babb JS et al (2006) Low-grade gliomas: dynamic susceptibility-weighted contrast-enhanced perfusion MR imaging-prediction of patient clinical response. *Radiology*. 238(2):658–667
36. Nguyen TB, Cron GO, Mercier JF et al (2015) Preoperative prognostic value of dynamic contrast-enhanced MRI-derived contrast transfer coefficient and plasma volume in patients with cerebral gliomas. *AJNR Am J Neuroradiol* 36(1):63–69. <https://doi.org/10.3174/ajnr.A4006>
37. Hlaihel C, Guilloton L, Guyotat J, Streichenberger N, Honnorat J, Cotton F (2010) Predictive value of multimodality MRI using conventional, perfusion, and spectroscopy MR in anaplastic transformation of low-grade oligodendrogliomas. *J Neurooncol* 97(1):73–80. <https://doi.org/10.1007/s11060-009-9991-4>
38. Law M, Young RJ, Babb JS et al (2008) Gliomas: predicting time to progression or survival with cerebral blood volume measurements at dynamic susceptibility-weighted contrast-enhanced perfusion MR imaging. *Radiology* 247(2):490–498. <https://doi.org/10.1148/radiol.2472070898>
39. Danchaiyittr N, Waldman AD, Tozer DJ et al (2008) Low-grade gliomas: do changes in rCBV measurements at longitudinal perfusion-weighted MR imaging predict malignant transformation? *Radiology* 247(1):170–178. <https://doi.org/10.1148/radiol.2471062089>
40. Back M, Jayamanne DT, Brazier D et al (2019) Influence of molecular classification in anaplastic glioma for determining outcome and future approach to management. *J Med Imaging Radiat Oncol* 63(2):272–280. <https://doi.org/10.1111/1754-9485.12850>
41. Shirahata M, Ono T, Stichel D et al (2018) Novel, improved grading system(s) for IDH-mutant astrocytic gliomas. *Acta Neuropathol* 136(1):153–166. <https://doi.org/10.1007/s00401-018-1849-4>
42. Patel SH, Poisson LM, Brat DJ et al (2017) T2-FLAIR mismatch, an imaging biomarker for IDH and 1p/19q status in lower-grade gliomas: a TCGA/TCIA

- project. *Clin Cancer Res* 23(20):6078–6085. <https://doi.org/10.1158/1078-0432.CCR-17-0560>
43. Ren Y, Zhang X, Rui W et al (2019) Noninvasive prediction of IDH1 mutation and ATRX expression loss in low-grade gliomas using multiparametric MR radiomic features. *J Magn Reson Imaging* 49(3):808–817. <https://doi.org/10.1002/jmri.26240>
  44. Hasselblatt M, Jaber M, Reuss D et al (2018) Diffuse astrocytoma, IDH-wildtype: a dissolving diagnosis. *J Neuropathol Exp Neurol* 77(6):422–425. <https://doi.org/10.1093/jnen/nly012>
  45. Brat DJ, Aldape K, Colman H, et al (2018) cIMPACT-NOW update 3: recommended diagnostic criteria for "diffuse astrocytic glioma, IDH-wildtype, with molecular features of glioblastoma, WHO grade IV. *Acta Neuropathol* 136(5):805–810, doi: <https://doi.org/10.1007/s00401-018-1913-0>
  46. Wu CC, Jain R, Radmanesh A et al (2018) Predicting genotype and survival in glioma using standard clinical MR imaging apparent diffusion coefficient images: a pilot study from the cancer genome atlas. *AJNR Am J Neuroradiol* 39(10):1814–1820. <https://doi.org/10.3174/ajnr. A5794>
  47. Smits M, van den Bent MJ (2017) Imaging correlates of adult glioma genotypes. *Radiology* 284(2):316–331. <https://doi.org/10.1148/radiol.2017151930>
  48. Leu K, Ott GA, Lai A et al (2017) Perfusion and diffusion MRI signatures in histologic and genetic subtypes of WHO grade II-III diffuse gliomas. *J Neurooncol* 134(1):177–188. <https://doi.org/10.1007/s11060-017-2506-9>
  49. Kickingereder P, Sahm F, Radbruch A et al (2015) IDH mutation status is associated with a distinct hypoxia/angiogenesis transcriptome signature which is non-invasively predictable with rCBV imaging in human glioma. *Sci Rep* 5:16238. <https://doi.org/10.1038/srep16238>
  50. Stadlbauer A, Zimmermann M, Kitzwögerer M et al (2017) MR imaging-derived oxygen metabolism and neovascularization characterization for grading and IDH gene mutation detection of gliomas. *Radiology* 283(3):799–809. <https://doi.org/10.1148/radiol.2016161422>
  51. Bian W, Khayal IS, Lupo JM et al (2009) Multiparametric characterization of grade 2 glioma subtypes using magnetic resonance spectroscopic, perfusion, and diffusion imaging. *Transl Oncol* 2(4):271–280
  52. Lin Y, Xing Z, She D et al (2017) IDH mutant and 1p/19q co-deleted oligodendrogliomas: tumor grade stratification using diffusion-, susceptibility-, and perfusion-weighted MRI. *Neuroradiology* 59(6):555–562. <https://doi.org/10.1007/s00234-017-1839-6>
  53. Yoon HJ, Ahn KJ, Lee S et al (2017) Differential diagnosis of oligodendroglial and astrocytic tumors using imaging results: the added value of perfusion MR imaging. *Neuroradiology* 59(7):665–675. <https://doi.org/10.1007/s00234-017-1851-x>
  54. Jenkinson MD, Smith TS, Joyce KA et al (2006) Cerebral blood volume, genotype and chemosensitivity in oligodendroglial tumours. *Neuroradiology* 48(10):703–713
  55. Chawla S, Kreja J, Vossough A et al (2013) Differentiation between oligodendroglioma genotypes using dynamic susceptibility contrast perfusion-weighted imaging and proton MR spectroscopy. *AJNR Am J Neuroradiol* 34(8):1542–1549. <https://doi.org/10.3174/ajnr. A3384>
  56. Emblem KE, Scheie D, Due-Tønnessen P et al (2008) Histogram analysis of MR imaging-derived cerebral blood volume maps: combined glioma grading and identification of low-grade oligodendroglial subtypes. *AJNR Am J Neuroradiol* 29(9):1664–1670. <https://doi.org/10.3174/ajnr. A1182>
  57. Emblem KE, Nedregaard B, Nome T et al (2008) Glioma grading by using histogram analysis of blood volume heterogeneity from MR-derived cerebral blood volume maps. *Radiology* 247(3):808–817. <https://doi.org/10.1148/radiol.2473070571>
  58. Dietrich O, Reiser MF, Schoenberg SO (2008) Artifacts in 3T MRI: physical background and reduction strategies. *Eur J Radiol* 65(1):29–35
  59. Vargas MI, Delavelle J, Kohler R, Becker CD, Lovblad K (2009) Brain and spine MRI artifacts at 3Tesla. *J Neuroradiol* 36(2):74–81. <https://doi.org/10.1016/j.neurad.2008.08.001>
  60. Kang Y, Choi SH, Kim YJ (2011) Gliomas: histogram analysis of apparent diffusion coefficient maps with standard- or high-b-value diffusion-weighted MR imaging—correlation with tumor grade. *Radiology* 261(3):882–890. <https://doi.org/10.1148/radiol.11110686>
  61. Zhou M, Scott J, Chaudhury B et al (2018) Radiomics in brain tumor: image assessment, quantitative feature descriptors, and machine-learning approaches. *AJNR Am J Neuroradiol* 39(2):208–216. <https://doi.org/10.3174/ajnr. A5391>
  62. Zhang X, Yan LF, Hu YC et al (2017) Optimizing a machine learning based glioma grading system using multi-parametric MRI histogram and texture features. *Oncotarget* 8(29):47816–47830. <https://doi.org/10.18632/oncotarget.18001>
  63. Lee MH, Kim J, Kim ST et al (2019) Prediction of IDH1 mutation in GBM using machine learning technique based on quantitative radiomic data. *World Neurosurg* 125:e688–e696. <https://doi.org/10.1016/j.wneu.2019.01.157>

## Publisher's Note

Springer Nature remains neutral with regard to jurisdictional claims in published maps and institutional affiliations.

**Submit your manuscript to a SpringerOpen<sup>®</sup> journal and benefit from:**

- Convenient online submission
- Rigorous peer review
- Open access: articles freely available online
- High visibility within the field
- Retaining the copyright to your article

---

Submit your next manuscript at ► [springeropen.com](https://www.springeropen.com)

---